Supporting Information for

Highly Thermostable Two–Dimensional Lanthanide(III) Metal–Organic Frameworks Constructed from 4, 4′, 4″-s-Triazine-2, 4, 6-triyl-tribenzoate Ligand: Synthesis, Structure, and Tunable White–Light Emission

Jiewei Rong,[a,b] Wenwei Zhang*[a] and Junfeng Bai*[a]

[a] *State Key Laboratory of Coordination Chemistry, School of Chemistry and Chemical Engineering, Nanjing University, Nanjing 210023, P. R. China. E–mail: wwzhang@nju.edu.cn, bjunfeng@nju.edu.cn*

[b]*School of Chemical and Materials Engineering, Huainan Normal University, Huainan, Anhui 232038, P. R. China. E–mail: zwj0076@126.com*

Table S1 Elemental analysis, yield and main IR bands for **1–8**

	Formula	C% (Found) [a]	H% (Found)	N% (Found)	Yield[b]	Main IR Bands
1	$C_{65}H_{75}La_2N_7O_{21}S_7$	43.55	4.22	5.47	65%	3417 m, 2998 w, 2914 w, 1602 s, 1563
		(43.44)	(4.09)	(5.29)		s, 1396 s, 1356 s, 1013 s, 814 m, 771 m
2	$C_{65}H_{75}Ce_2N_7O_{21}S_7$	43.49	4.21	5.46	70%	3425 m, 3016 w, 2914 w, 1594 s, 1558
		(43.36)	(4.12)	(5.38)		s, 1396 s, 1356 s, 1013 s, 823 m, 770 m
3	$C_{65}H_{75}Pr_2N_7O_{21}S_7$	43.45	4.21	5.46	68%	3447 m, 3007 w, 2914 w, 1598 s, 1554
		(43.25)	(4.05)	(5.25)		s, 1396 s, 1356 s, 1013 s, 819 m, 771 m
4	$C_{65}H_{75}Sm_2N_7O_{21}S_7$	43.00	4.16	5.40	75%	3421 m, 2998 w, 2914 w, 1594 s, 1554
		(42.85)	(3.97)	(5.41)		s, 1396 s, 1352 s, 1013 s, 814 m, 775 m
5	$C_{65}H_{75}Eu_2N_7O_{21}S_7$	42.93	4.16	5.39	78%	3408 m, 2998 w, 2910 w, 1602 s, 1558
		(42.75)	(3.92)	(5.48)		s, 1396 s, 1352 s, 1013 s, 823 m, 771 m
6	$C_{64}H_{75}Nd_2N_7O_{22}S_6$	43.30	4.26	5.52	75%	3412 m, 2998 w, 2910 w, 1602 s, 1558
		(43.02)	(4.12)	(5.49)		s, 1400 s, 1356 s, 1013 s, 819 m, 766 m
7	$C_{64}H_{75}Gd_2N_7O_{22}S_6$	42.68	4.20	5.44	76%	3416 m, 3002 w, 2906 w, 1602 s, 1545
		(42.41)	(4.01)	(5.24)		s, 1396 s, 1356 s, 1014 s, 823 m, 779 m
8	$C_{64}H_{75}Tb_2N_7O_{22}S_6$	42.60	4.19	5.43	64%	3421 m, 3002 w, 2914 w, 1594 s, 1554
		(42.32)	(3.82)	(5.49)		s, 1400 s, 1352 s, 1018 s, 828 m, 771 m

[a]Calculated value from formula, followed by experimental value in parentheses. [b]Yield was calculated based on rare earth metal.

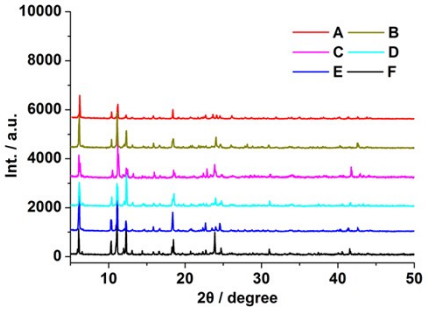

Fig. S1 The PXRD patterns for complex **La–TATB** (**F**) and the codoped complexes $\mathbf{Eu_xTb_yLa_{1-x-y}}$**–TATB**, **A**–**E** (Eu, Tb, La%): **A** (25, 4.5, 70.5), **B** (24.5, 4, 71.5), **C** (25.5, 3.5, 71), **D (24, 3, 73)**, and **E** (23.5, 2, 74.5).

Table S2 Elemental analysis for the co−doped compounds

Ln–TATB	Wt% C	Wt% H	Wt% N
	Calcd (Found)	Calcd (Found)	Calcd (Found)
$Eu_{0.25}Tb_{0.045}La_{0.705}$–TATB	43.35 (43.43)	4.20 (4.10)	5.44 (5.34)
$Eu_{0.245}Tb_{0.04}La_{0.715}$–TATB	43.36 (43.45)	4.20 (4.09)	5.45 (5.31)
$Eu_{0.255}Tb_{0.035}La_{0.71}$–TATB	43.36 (43.44)	4.20 (4.12)	5.45 (5.28)
$Eu_{0.24}Tb_{0.03}La_{0.73}$–TATB	43.37 (43.45)	4.20 (4.07)	5.45 (5.24)
$Eu_{0.235}Tb_{0.02}La_{0.745}$–TATB	43.37 (43.44)	4.20 (4.16)	5.45 (5.27)

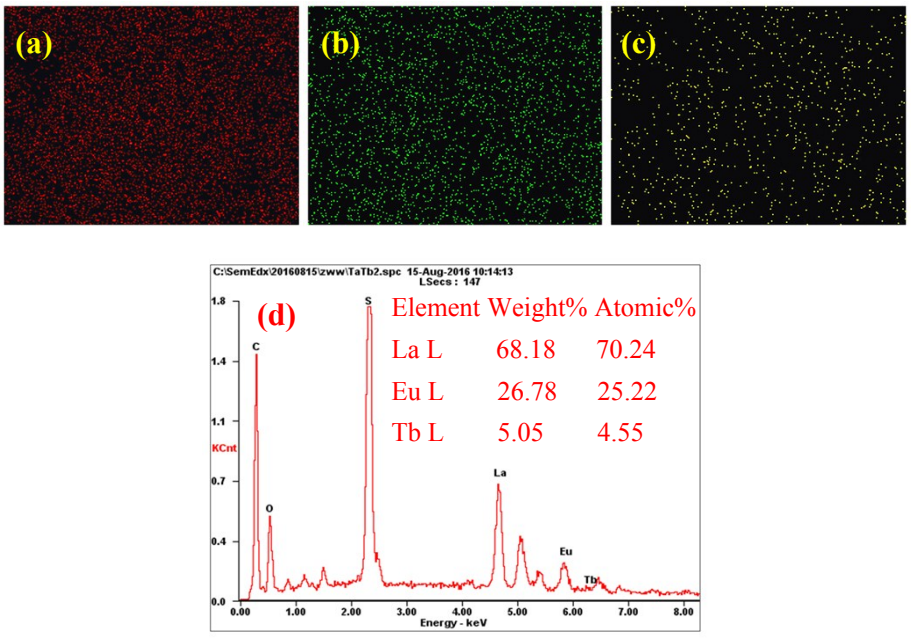

Fig. S2 (a, b, c) Elemental mapping images of **$Eu_{0.25}Tb_{0.045}La_{0.705}$–TATB** (red, green and yellow dots represent the La, Eu and Tb elements, respectively) and (d) EDX−spectra of **$Eu_{0.25}Tb_{0.045}La_{0.705}$–TATB**.

Table S3 Crystallographic data and structural refinements for **2**, **3**, **4**, **6** and **7**

Compound	**2**	**3**	**4**	**6**	**7**
Formula	$C_{65}H_{75}Ce_2N_7O_{21}S_7$	$C_{65}H_{75}Pr_2N_7O_{21}S_7$	$C_{65}H_{75}Sm_2N_7O_{21}S_7$	$C_{64}H_{75}Nd_2N_7O_{22}S_6$	$C_{64}H_{75}Gd_2N_7O_{22}S_6$
Formula weight	1795.00	1796.60	1815.50	1775.18	1801.20
Temperature (K)	293(2)	293(2)	293(2)	293(2)	293(2)
Crystal system	Triclinic	Triclinic	Triclinic	Triclinic	Triclinic
Space group	*P–1*	*P–1*	*P–1*	*P–1*	*P–1*
a (Å)	16.1339(6)	16.1230(8)	16.0585(7)	16.0917(6)	16.0579(7)
b (Å)	16.3437(6)	16.3385(8)	16.3646(7)	16.3567(6)	16.2365(7)
c (Å)	17.2177(6)	17.2058(8)	17.1438(7)	17.1769(6)	17.1282(8)
α (deg)	111.1013(10)	110.6340(10)	110.3627(7)	110.7240(10)	109.6540(10)
β (deg)	110.6951(10)	110.9040(10)	111.0098(7)	110.8480(10)	111.3560(10)
γ (deg)	96.1766(12)	96.3680(10)	96.5967(8)	96.3870(10)	96.9450(10)
V (Å^3)	3816.2(2)	3814.6(3)	3792.2(3)	3803.4(2)	3762.9(3)
Z	2	2	1	2	2
F(000)	1636	1640	1628	1596	1612
GOF	1.148	0.965	1.123	1.096	1.105
R_1,wR_2	0.0548, 0.1619	0.0500, 0.1496	0.0502, 0.1567	0.0531, 0.1658	0.0545, 0.1762
[$I > 2\sigma(I)$] [a]					

[a] $R_1 = \Sigma||F_0|-|F_c||/\Sigma|F_0|$, w$R_2 = \{\Sigma[w(F_0^2-F_c^2)^2]/\Sigma[w(F_0^2)^2]\}^{1/2}$

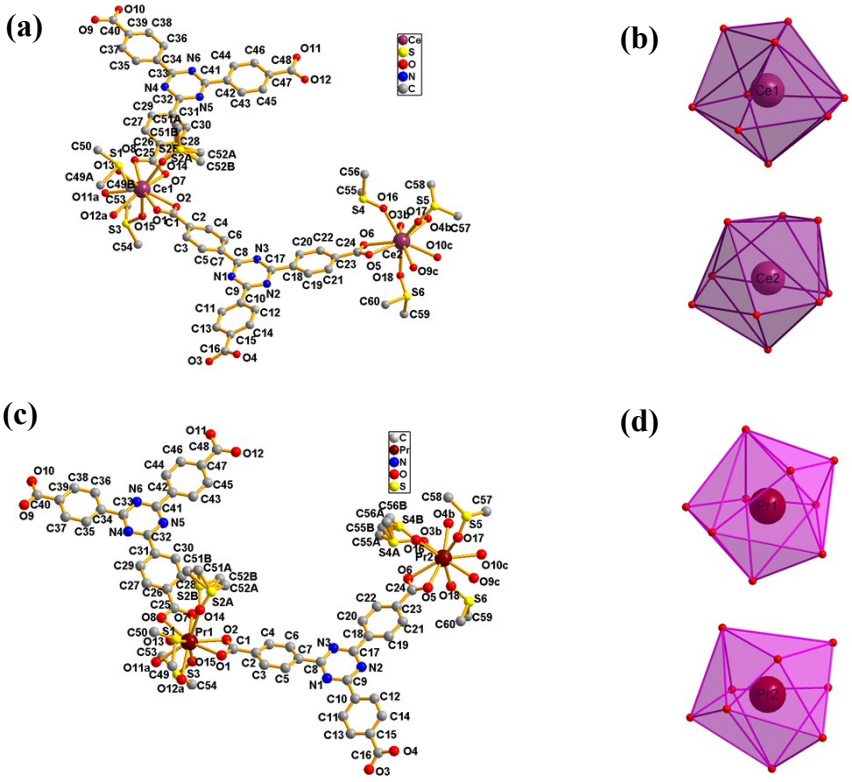

(e)

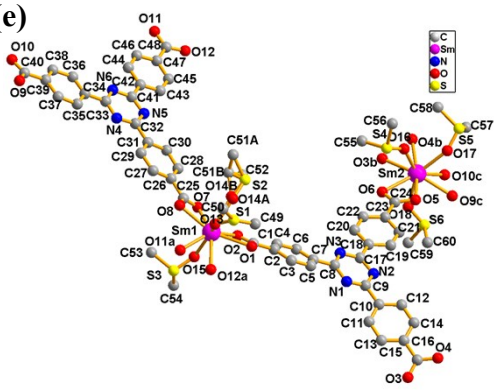
C
Sm
N
O
S
Sm1
Sm2

(f)

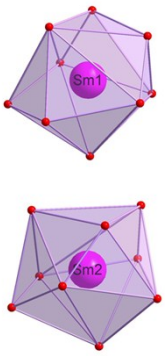
Sm1
Sm2

(g)

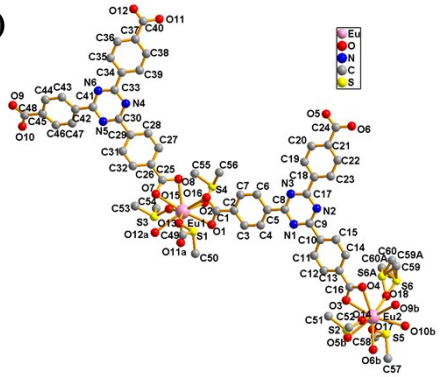
Eu
O
N
C
S
Eu1
Eu2

(h)

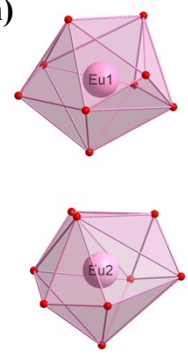
Eu1
Eu2

(i)

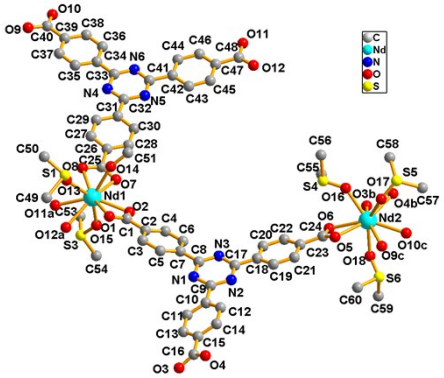
C
Nd
N
O
S
Nd1
Nd2

(j)

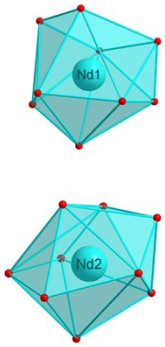
Nd1
Nd2

(k)

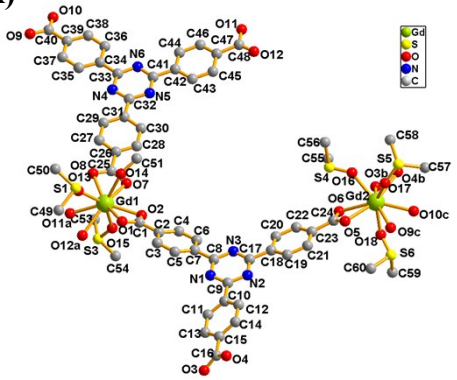
Gd
S
O
N
C
Gd1
Gd2

(l)

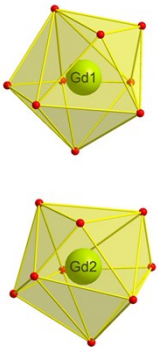
Gd1
Gd2

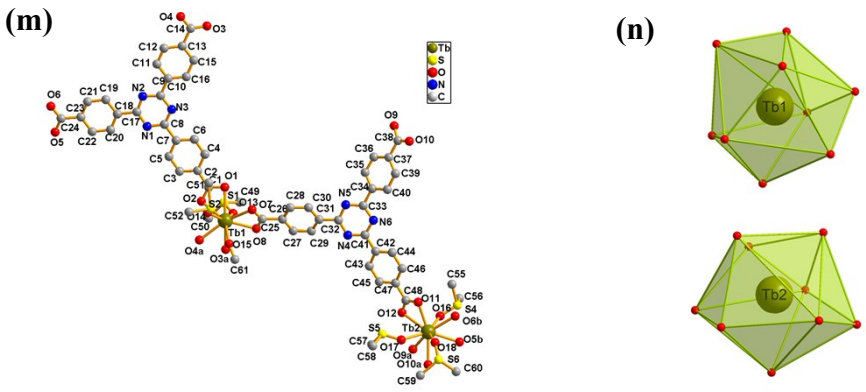

Fig. S3 (a) Coordination environments of Ce^{3+} ions with the H atoms omitted for clarity; symmetry codes: a = x, y, 1+z; b = x, y, –1+z; c = –2+x, –1+y, –1+ z; (b) Coordination polyhedron of Ce^{3+} ions; (c) Coordination environments of Pr^{3+} ions with the H atoms omitted for clarity; symmetry codes: a = x, y, 1+z; b = x, y, –1+z; c = –2+x, –1+y, –1+z; (d) Coordination polyhedron of Pr^{3+} ions; (e) Coordination environments of Sm^{3+} ions with the H atoms omitted for clarity; symmetry codes: a = x, y, 1+z; b = x, y, –1+z; c = –2+x, –1+y, –1+ z; (f) Coordination polyhedron of Sm^{3+} ions; (g) Coordination environments of Eu^{3+} ions with the H atoms omitted for clarity; symmetry codes: a = x, y, –1+z; b = 2+x, 1+y, z; (h) Coordination polyhedron of Eu^{3+} ions; (i) Coordination environments of Nd^{3+} ions with the H atoms omitted for clarity; symmetry codes: a = x, y, 1+z; b = x, y, –1+z; c = –2+x, –1+y, –1+ z; (j) Coordination polyhedron of Nd^{3+} ions; (k) Coordination environments of Gd^{3+} ions with the H atoms omitted for clarity; symmetry codes: a = x, y, 1+z; b = x, y, –1+z; c = –2+x, –1+y, –1+ z; (l) Coordination polyhedron of Gd^{3+} ions; (m) Coordination environments of Tb^{3+} ions with the H atoms omitted for clarity; symmetry codes: a = x, y, 1+z; b = 2+x, 1+y, z; (n) Coordination polyhedron of Tb^{3+} ions.

Table S4 Selected bond distances (Å) in **1–8**

			1		
La1–O15	2.473(9)	La1–O14	2.484(10)	La1–O13	2.497(9)
La1– O2	2.534(7)	La1–O7	2.565(7)	La1–O11	2.576(6)
La1–O8	2.613(7)	La1–O12	2.628(6)	La1–O1	2.670(7)
La2–O16	2.488(7)	La2–O18	2.494(8)	La2–O17	2.494(9)
La2–O5	2.555(6)	La2–O4	2.579(7)	La2–O10	2.587(6)
La2–O9	2.603(6)	La2–O3	2.641(8)	La2–O6	2.689(7)
			2		
Ce1–O13	2.460(5)	Ce1–O15	2.478(4)	Ce1–O14	2.491(5)
Ce1–O2	2.526(4)	Ce1–O11	2.538(4)	Ce1–O7	2.547(4)
Ce1–O8	2.586(4)	Ce1–O12	2.603(4)	Ce1–O1	2.632(4)
Ce2–O16	2.470(4)	Ce2–O18	2.482(4)	Ce2–O17	2.486(4)
Ce2–O5	2.543(3)	Ce2–O4	2.554(4)	Ce2–O10	2.564(3)
Ce2–O9	2.576(3)	Ce2–O3	2.578(4)	Ce2–O6	2.668(4)
			3		
Pr1–O13	2.450(4)	Pr1–O15	2.453(4)	Pr1–O14	2.481(5)
Pr1–O2	2.501(4)	Pr1–O11	2.532(3)	Pr1–O7	2.533(4)
Pr1–O8	2.552(4)	Pr1–O12	2.589(4)	Pr1–O1	2.622(4)
Pr2–O16	2.448(4)	Pr2–O18	2.464(4)	Pr2–O17	2.467(4)
Pr2–O5	2.518(3)	Pr2–O4	2.532(4)	Pr2–O10	2.548(3)
Pr2–O3	2.548(4)	Pr2–O9	2.561(3)	Pr2–O6	2.665(4)
			4		
Sm1–O13	2.398(5)	Sm1–O15	2.414(5)	Sm1–O14	2.424(2)
Sm1–O2	2.452(5)	Sm1–O11	2.473(4)	Sm1–O7	2.498(4)
Sm1–O8	2.517(4)	Sm1–O12	2.549(4)	Sm1–O1	2.588(4)
Sm2–O16	2.410(5)	Sm2–O17	2.421(5)	Sm2–O18	2.425(4)
Sm2–O5	2.471(4)	Sm2–O4	2.499(4)	Sm2–O10	2.502(4)
Sm2–O9	2.517(4)	Sm2–O3	2.523(4)	Sm2–O6	2.643(4)
			5		
Eu1–O15	2.390(5)	Eu1–O13	2.414(5)	Eu1–O16	2.429(6)
Eu1–O11	2.451(5)	Eu1–O2	2.490(5)	Eu1–O8	2.495(5)
Eu1–O7	2.503(5)	Eu1–O1	2.504(5)	Eu1–O12	2.642(5)
Eu2–O17	2.389(6)	Eu2–O14	2.405(6)	Eu2–O18	2.411(7)
Eu2–O9	2.438(5)	Eu2–O5	2.473(5)	Eu2–O4	2.490(5)
Eu2–O3	2.501(5)	Eu2–O6	2.531(5)	Eu2–O10	2.580(5)
			6		
Nd1–O13	2.422(5)	Nd1–O15	2.432(4)	Nd1–O14	2.467(5)
Nd1–O2	2.481(4)	Nd1–O11	2.509(4)	Nd1–O7	2.525(4)
Nd1–O8	2.544(4)	Nd1–O12	2.568(4)	Nd1–O1	2.611(4)
Nd2–O16	2.431(4)	Nd2–O17	2.450(4)	Nd2–O18	2.455(4)
Nd2–O5	2.499(4)	Nd2–O4	2.523(4)	Nd2–O10	2.530(3)
Nd2–O3	2.537(4)	Nd2–O9	2.543(3)	Nd2–O6	2.657(4)

			7		
Gd1–O13	2.348(5)	Gd1–O15	2.393(5)	Gd1–O14	2.403(6)
Gd1–O2	2.415(5)	Gd1–O11	2.463(4)	Gd1–O7	2.468(4)
Gd1–O8	2.493(4)	Gd1–O12	2.513(4)	Gd1–O1	2.575(4)
Gd2–O16	2.378(4)	Gd2–O18	2.397(4)	Gd2–O17	2.403(5)
Gd2–O5	2.439(4)	Gd2–O10	2.465(4)	Gd2–O3	2.476(4)
Gd2–O4	2.484(5)	Gd2–O9	2.487(4)	Gd2–O6	2.635(4)
			8		
Tb1–O14	2.354(5)	Tb1–O13	2.377(5)	Tb1–O8	2.400(5)
Tb1–O15	2.401(6)	Tb1–O2	2.447(5)	Tb1–O3	2.464(5)
Tb1–O4	2.477(5)	Tb1–O1	2.505(5)	Tb1–O7	2.576(5)
Tb2–O17	2.380(5)	Tb2–O18	2.391(5)	Tb2–O16	2.396(5)
Tb2–O11	2.432(5)	Tb2–O5	2.456(4)	Tb2–O10	2.459(5)
Tb2–O9	2.463(5)	Tb2–O6	2.476(4)	Tb2–O12	2.633(5)

Table S5 Selected bond angles (°) in **1–8**

		1	
O15–La1–O14	145.7(3)	O15–La1–O13	142.2(3)
O14–La1–O13	71.7(4)	O15–La1–O2	74.9(3)
O14–La1–O2	80.1(4)	O13–La1–O2	133.8(3)
O15–La1–O7	76.7(3)	O14–La1–O7	74.1(3)
O13–La1–O7	128.7(3)	O2–La1–O7	73.9(2)
O15–La1–O11	72.7(3)	O14–La1–O11	135.2(3)
O13– La1–O11	71.8(3)	O2–La1–O11	144.7(3)
O7–La1–O11	111.1(2)	O15–La1–O8	92.9(3)
O14–La1–O8	81.7(4)	O13–La1–O8	88.1(3)
O2–La1–O8	123.7(2)	O7–La1–O8	49.8(2)
O11–La1–O8	71.8(2)	O15–La1–O12	75.1(3)
O14–La1–O12	135.9(3)	O13–La1–O12	72.5(3)
O2–La1–O12	107.9(3)	O7–La1–O12	150.0(3)
O11–La1–O12	50.0(2)	O8–La1–O12	121.8(2)
O15–La1–O1	98.8(3)	O14–La1–O1	82.6(3)
O13–La1–O1	89.1(3)	O2–La1–O1	50.7(3)
O7–La1–O1	122.9(2)	O11–La1–O1	121.8(2)
O8–La1–O1	164.2(3)	O12–La1–O1	71.9(2)
O16–La2–O18	145.5(3)	O16–La2–O17	69.2(3)
O18–La2–O17	143.4(3)	O16–La2–O5	79.5(3)
O18–La2–O5	80.7(3)	O17–La2–O5	103.3(3)
O16–La2–O4	86.3(3)	O18–La2–O4	108.2(3)
O17–La2–O4	77.7(3)	O5–La2–O4	164.3(2)
O16–La2–O10	140.3(3)	O18–La2–O10	74.0(3)
O17–La2–O10	73.6(3)	O5–La2–O10	123.2(2)
O4–La2–O10	72.4(2)	O16–La2–O9	126.2(3)

O18–La2–O9	73.5(2)	O17–La2–O9	72.9(3)
O5–La2–O9	73.62(19)	O4–La2–O9	120.96(19)
O10–La2–O9	50.75(19)	O16–La2–O3	76.9(3)
O18–La2–O3	88.6(3)	O17–La2–O3	118.8(3)
O5–La2–O3	118.8(2)	O4–La2–O3	50.3(2)
O10–La2–O3	110.6(2)	O9–La2–O3	156.6(3)
O16–La2–O6	71.9(3)	O18–La2–O6	73.7(3)
O17–La2–O6	136.2(3)	O5–La2–O6	49.7(2)
O4–La2–O6	119.2(2)	O10–La2–O6	147.8(3)
O9–La2–O6	117.58(19)	O3–La2–O6	69.4(2)
		2	
O13–Ce1–O15	142.88(15)	O13–Ce1–O14	72.06(19)
O15–Ce1–O14	144.78(17)	O13–Ce1–O2	133.81(16)
O15–Ce1–O2	74.93(16)	O14–Ce1–O2	78.8(2)
O13–Ce1–O11	72.11(15)	O15–Ce1–O11	72.91(14)
O14–Ce1–O11	136.02(18)	O2–Ce1–O11	145.20(16)
O13–Ce1–O7	127.95(16)	O15–Ce1–O7	76.78(16)
O14–Ce1–O7	73.57(18)	O2–Ce1–O7	73.57(13)
O11–Ce1–O7	111.02(13)	O13–Ce1–O8	86.98(16)
O15–Ce1–O8	93.35(15)	O14–Ce1–O8	82.20(18)
O2–Ce1–O8	123.89(13)	O11–Ce1–O8	71.28(12)
O7–Ce1–O8	50.43(12)	O13–Ce1–O12	73.06(16)
O15–Ce1–O12	75.43(15)	O14–Ce1–O12	135.92(17)
O2–Ce1–O12	108.09(14)	O11–Ce1–O12	50.71(11)
O7–Ce1–O12	150.51(16)	O8–Ce1–O12	121.82(11)
O13–Ce1–O1	89.36(15)	O15–Ce1–O1	100.05(15)
O14– Ce1– O1	80.03(18)	O2–Ce1–O1	50.22(13)
O11–Ce1–O1	123.96(12)	O7–Ce1–O1	121.42(12)
O8–Ce1–O1	162.13(14)	O12–Ce1–O1	73.46(12)
O16–Ce2–O18	145.77(13)	O16–Ce2–O17	69.32(14)
O18–Ce2–O17	143.14(14)	O16–Ce2–O5	80.27(14)
O18–Ce2–O5	80.86(14)	O17–Ce2–O5	102.52(14)
O16–Ce2–O4	84.24(14)	O18–Ce2–O4	109.54(14)
O17–Ce2–O4	77.16(15)	O5–Ce2–O4	163.45(13)
O16–Ce2–O10	139.76(14)	O18–Ce2–O10	74.16(14)
O17–Ce2–O10	73.83(14)	O5–Ce2–O10	123.92(11)
O4–Ce2–O10	72.19(11)	O16–Ce2–O9	127.43(14)
O18–Ce2–O9	73.33(13)	O17–Ce2 –O9	72.47(14)
O5–Ce2–O9	74.24(11)	O4–Ce2– O9	120.51(11)
O10–Ce2–O9	50.84(11)	O16 –Ce2 –O3	78.22(15)
O18–Ce2–O3	86.86(14)	O17 –Ce2– O3	120.34(14)
O5–Ce2–O3	119.86(11)	O4–Ce2–O3	50.35(11)
O10–Ce2–O3	108.08(13)	O9–Ce2–O3	153.97(15)
O16–Ce2–O6	72.39(14)	O18–Ce2–O6	73.60(14)

O17–Ce2–O6	136.09(14)	O5–Ce2–O6	49.68(11)
O4–Ce2–O6	119.56(11)	O10–Ce2–O6	147.76(14)
O9–Ce2–O6	117.91(11)	O3–Ce2–O6	70.33(11)
		3	
O13–Pr1–O15	143.16(16)	O13–Pr1–O14	72.19(19)
O15–Pr1–O14	144.35(18)	O13–Pr1–O2	133.88(17)
O15–Pr1–O2	74.87(16)	O14–Pr1–O2	78.4(2)
O13–Pr1–O11	72.32(15)	O15–Pr1–O11	72.90(13)
O14–Pr1–O11	136.39(19)	O2–Pr1–O11	145.17(16)
O13–Pr1–O7	127.97(17)	O15–Pr1–O7	76.27(16)
O14–Pr1–O7	73.79(19)	O2–Pr1–O7	73.52(13)
O11–Pr1–O7	110.64(13)	O13–Pr1–O8	85.95(17)
O15–Pr1–O8	94.17(17)	O14–Pr1–O8	81.7(2)
O2–Pr1–O8	124.26(13)	O11–Pr1–O8	71.30(12)
O7–Pr1–O8	50.95(12)	O13–Pr1–O12	73.78(16)
O15–Pr1–O12	75.27(15)	O14–Pr1–O12	136.18(18)
O2–Pr1–O12	107.52(14)	O11–Pr1–O12	51.30(11)
O7–Pr1–O12	150.02(16)	O8–Pr1–O12	122.39(12)
O13–Pr1–O1	89.11(16)	O15–Pr1–O1	100.46(15)
O14–Pr1–O1	79.71(19)	O2–Pr1–O1	50.60(13)
O11–Pr1–O1	124.00(11)	O7–Pr1–O1	121.76(13)
O8–Pr1–O1	161.40(15)	O12–Pr1–O1	72.97(12)
O16–Pr2–O18	145.27(14)	O16–Pr2–O17	69.74(15)
O18–Pr2–O17	143.18(14)	O16–Pr2–O5	80.33(14)
O18–Pr2–O5	81.37(14)	O17–Pr2–O5	101.10(15)
O16–Pr2–O4	82.66(15)	O18–Pr2–O4	110.83(15)
O17–Pr2–O4	77.02(16)	O5–Pr2–O4	162.40(13)
O16–Pr2–O10	139.65(14)	O18–Pr2–O10	74.56(14)
O17–Pr2–O10	74.09(14)	O5–Pr2–O10	124.49(11)
O4–Pr2–O10	72.24(11)	O16–Pr2–O3	78.47(15)
O18–Pr2–O3	85.69(14)	O17–Pr2–O3	121.88(15)
O5–Pr2–O3	120.19(12)	O4–Pr2–O3	51.12(12)
O10–Pr2–O3	107.10(12)	O16–Pr2–O9	128.09(14)
O18–Pr2–O9	73.58(13)	O17–Pr2–O9	71.95(14)
O5–Pr2–O9	74.11(11)	O4–Pr2–O9	120.76(11)
O10–Pr2–O9	51.42(11)	O3–Pr2–O9	153.12(14)
O16–Pr2–O6	72.43(14)	O18–Pr2–O6	73.16(14)
O17–Pr2–O6	135.84(14)	O5–Pr2–O6	50.11(11)
O4–Pr2–O6	119.70(11)	O10–Pr2–O6	147.73(13)
O3–Pr2–O6	70.21(11)	O9–Pr2–O6	117.82(11)
		4	
O13–Sm1–O15	143.66(17)	O13–Sm1–O14	70.4(4)
O15–Sm1–O14	145.7(4)	O13–Sm1–O2	134.53(18)
O15–Sm1–O2	73.91(18)	O14–Sm1–O2	79.7(6)

O13–Sm1–O11	72.41(17)	O15–Sm1–O11	73.08(16)
O14–Sm1–O11	136.1(6)	O2–Sm1–O11	144.20(18)
O13–Sm1–O7	127.94(18)	O15–Sm1–O7	75.75(17)
O14–Sm1–O7	76.0(4)	O2–Sm1–O7	73.31(15)
O11–Sm1–O7	111.05(15)	O13–Sm1–O8	84.77(18)
O15–Sm1–O8	95.12(18)	O14–Sm1–O8	82.2(6)
O2–Sm1–O8	124.79(16)	O11–Sm1–O8	71.89(15)
O7–Sm1–O8	51.74(14)	O13–Sm1–O12	74.60(18)
O15–Sm1–O12	75.37(16)	O14–Sm1–O12	134.0(4)
O2–Sm1–O12	106.14(16)	O11–Sm1–O12	51.80(13)
O7–Sm1–O12	149.96(17)	O8–Sm1–O12	123.42(14)
O13–Sm1–O1	87.57(17)	O15–Sm1–O1	102.68(17)
O14–Sm1–O1	76.6(6)	O2–Sm1–O1	51.88(16)
O11–Sm1–O1	124.20(14)	O7–Sm1–O1	121.85(15)
O8–Sm1–O1	158.82(18)	O12–Sm1–O1	72.94(14)
O16–Sm2–O17	70.34(17)	O16–Sm2–O18	144.26(16)
O17–Sm2–O18	143.59(16)	O16–Sm2–O5	80.76(16)
O17–Sm2–O5	99.00(17)	O18–Sm2–O5	81.96(17)
O16–Sm2–O4	80.24(17)	O17–Sm2–O4	77.47(17)
O18–Sm2–O4	112.27(17)	O5–Sm2–O4	160.75(16)
O16–Sm2–O10	139.86(16)	O17–Sm2–O10	75.28(17)
O18–Sm2–O10	74.82(16)	O5–Sm2–O10	125.33(13)
O4–Sm2–O10	72.53(14)	O16–Sm2–O9	129.55(16)
O17–Sm2–O9	71.43(16)	O18–Sm2–O9	73.98(15)
O5–Sm2–O9	74.03(13)	O4–Sm2–O9	121.37(14)
O10–Sm2–O9	52.29(13)	O16–Sm2–O3	78.71(18)
O17–Sm2–O3	123.78(16)	O18–Sm2–O3	83.95(16)
O5–Sm2–O3	121.20(14)	O4–Sm2–O3	51.33(14)
O10–Sm2–O3	104.84(15)	O9– Sm2 –O3	151.41(16)
O16–Sm2–O6	72.13(16)	O17–Sm2–O6	134.94(17)
O18–Sm2–O6	72.69(16)	O5–Sm2–O6	50.66(13)
O4–Sm2–O6	119.37(13)	O10–Sm2–O6	147.49(16)
O9–Sm2–O6	117.89(13)	O3–Sm2–O6	70.62(14)
		5	
O15–Eu1–O13	144.16(19)	O15–Eu1–O16	70.5(2)
O13–Eu1–O16	143.4(19)	O15–Eu1–O11	80.50(19)
O13–Eu1–O11	82.30(18)	O16–Eu1–O11	98.3(2)
O15–Eu1–O2	139.62(19)	O13–Eu1–O2	75.06(19)
O16–Eu1–O2	75.3(2)	O11–Eu1–O2	125.92(16)
O15–Eu1–O8	79.7(2)	O13–Eu1–O8	113.0(2)
O16–Eu1–O8	77.4(2)	O11–Eu1–O8	160.05(19)
O2–Eu1–O8	72.28(17)	O15–Eu1–O7	79.0(2)
O13–Eu1–O7	83.53(19)	O16–Eu1–O7	124.6(2)
O11–Eu1–O7	121.24(18)	O2–Eu1–O7	104.32(17)

O8–Eu1–O7	51.95(18)	O15–Eu1–O1	129.90(19)
O13–Eu1–O1	73.85(18)	O16–Eu1–O1	71.19(19)
O11–Eu1–O1	74.33(16)	O2–Eu1–O1	52.47(15)
O8–Eu1–O1	121.16(17)	O7–Eu1–O1	150.80(18)
O15–Eu1–O12	72.29(19)	O13–Eu1–O12	72.47(18)
O16–Eu1–O12	134.79(19)	O11–Eu1–O12	50.57(16)
O2–Eu1–O12	147.50(18)	O8–Eu1–O12	119.82(17)
O7–Eu1–O12	70.77(17)	O1–Eu1–O12	117.73(16)
O17–Eu2–O14	144.1(2)	O17–Eu2–O18	72.9(3)
O14–Eu2–O18	142.6(3)	O17–Eu2–O9	134.0(2)
O14–Eu2–O9	73.9(2)	O18–Eu2–O9	78.8(3)
O17–Eu2–O5	72.3(2)	O14–Eu2–O5	73.60(18)
O18–Eu2–O5	136.7(3)	O9–Eu2–O5	144.5(2)
O17–Eu2–O4	128.2(2)	O14–Eu2–O4	75.2(2)
O18–Eu2–O4	73.0(3)	O9–Eu2–O4	73.8(2)
O5–Eu2–O4	110.85(19)	O17–Eu2–O3	84.5(2)
O14–Eu2–O3	95.5(2)	O18–Eu2–O3	79.9(3)
O9–Eu2–O3	125.39(19)	O5–Eu2–O3	71.87(18)
O4–Eu2–O3	51.96(18)	O17–Eu2–O6	74.5(2)
O14–Eu2–O6	75.88(19)	O18–Eu2–O6	136.9(3)
O9–Eu2–O6	105.55(19)	O5–Eu2–O6	52.33(16)
O4–Eu2–O6	150.0(2)	O3–Eu2–O6	123.88(17)
O17–Eu2–O10	87.0(2)	O14–Eu2–O10	103.3(2)
O18–Eu2–O10	78.0(3)	O9–Eu2–O10	51.60(19)
O5–Eu2–O10	124.56(17)	O4–Eu2–O10	121.90(18)
O3–Eu2–O10	157.9(2)	O6–Eu2–O10	72.88(17)
		6	
O13–Nd1–O15	143.77(17)	O13–Nd1–O14	72.3(2)
O15–Nd1–O14	143.55(18)	O13–Nd1–O2	133.79(17)
O15–Nd1–O2	74.42(17)	O14–Nd1–O2	78.7(2)
O13–Nd1–O11	72.59(16)	O15–Nd1–O11	73.10(14)
O14–Nd1–O11	136.59(18)	O2–Nd1–O11	144.68(17)
O13–Nd1–O7	127.79(17)	O15–Nd1–O7	76.13(16)
O14–Nd1–O7	72.9(2)	O2–Nd1–O7	73.51(14)
O11–Nd1–O7	111.17(14)	O13–Nd1–O8	85.97(17)
O15–Nd1–O8	94.06(17)	O14–Nd1–O8	81.2(2)
O2–Nd1–O8	124.44(14)	O11–Nd1–O8	71.62(13)
O7–Nd1–O8	51.10(13)	O13–Nd1–O12	74.32(17)
O15–Nd1–O12	75.41(15)	O14–Nd1–O12	136.87(19)
O2–Nd1–O12	106.78(15)	O11–Nd1–O12	51.35(12)
O7–Nd1–O12	150.21(16)	O8–Nd1–O12	122.79(13)
O13–Nd1–O1	88.19(16)	O15–Nd1–O1	101.64(16)
O14–Nd1–O1	79.19(19)	O2–Nd1–O1	50.95(14)
O11–Nd1–O1	124.13(12)	O7–Nd1–O1	121.53(13)

O8–Nd1–O1	160.39(16)	O12–Nd1–O1	73.17(13)
O16–Nd2–O17	70.03(15)	O16–Nd2–O18	144.77(15)
O17–Nd2–O18	143.39(14)	O16–Nd2–O5	80.41(15)
O17–Nd2–O5	100.02(15)	O18–Nd2–O5	81.77(14)
O16–Nd2–O4	81.92(15)	O17–Nd2–O4	77.43(15)
O18–Nd2–O4	111.13(15)	O5–Nd2–O4	161.91(13)
O16–Nd–O10	139.90(14)	O17–Nd2–O10	74.55(14)
O18–Nd2–O10	74.64(14)	O5–Nd2–O10	124.54(12)
O4–Nd2–O10	72.46(12)	O16–Nd2–O3	78.60(16)
O17–Nd2–O3	122.73(15)	O18–Nd2–O3	84.86(14)
O5–Nd2–O3	120.75(13)	O4–Nd2–O3	51.11(13)
O10–Nd2–O3	106.37(13)	O16–Nd2–O9	128.63(14)
O17–Nd2–O9	71.55(15)	O18 –Nd2– O9	73.95(14)
O5–Nd2–O9	74.09(12)	O4–Nd2–O9	120.84(12)
O10–Nd2–O9	51.46(11)	O3–Nd2–O9	152.42(14)
O16–Nd2–O6	72.23(14)	O17–Nd2–O6	135.36(14)
O18–Nd2–O6	72.98(14)	O5–Nd2–O6	50.34(12)
O4–Nd2–O6	119.69(12)	O10–Nd2–O6	147.61(14)
O3–Nd2–O6	70.53(12)	O9–Nd2–O6	117.88(12)
		7	
O13–Gd1–O15	144.17(18)	O13–Gd1–O14	74.6(2)
O15–Gd1–O14	140.81(19)	O13–Gd1–O2	134.55(18)
O15–Gd1–O2	73.33(18)	O14–Gd1–O2	77.9(2)
O13–Gd1–O11	72.53(18)	O15–Gd1–O11	73.37(16)
O14–Gd1–O11	138.41(19)	O2–Gd1–O11	143.60(18)
O13–Gd1–O7	128.26(17)	O15–Gd1–O7	74.53(18)
O14–Gd1–O7	72.3(2)	O2–Gd1–O7	74.10(16)
O11–Gd1–O7	110.28(17)	O13–Gd1–O8	83.33(18)
O15–Gd1–O8	96.53(19)	O14–Gd1–O8	79.3(2)
O2–Gd1–O8	125.93(16)	O11–Gd1–O8	72.31(15)
O7–Gd1–O8	52.35(15)	O13–Gd1–O12	74.39(18)
O15–Gd1–O12	76.41(16)	O14–Gd1–O12	137.70(19)
O2–Gd1–O12	105.10(16)	O11–Gd1–O12	52.52(13)
O7–Gd1–O12	149.81(18)	O8–Gd1–O12	124.30(15)
O13–Gd1–O1	86.94(17)	O15–Gd1–O1	103.60(18)
O14–Gd1–O1	77.9(2)	O2–Gd1–O1	51.98(16)
O11–Gd1–O1	124.40(14)	O7–Gd1–O1	122.50(16)
O8–Gd1–O1	156.81(19)	O12–Gd1–O1	72.46(15)
O16–Gd2–O18	143.45(17)	O16–Gd2–O17	70.59(17)
O18–Gd2–O17	143.98(16)	O16–Gd2–O5	81.15(16)
O18–Gd2–O5	82.23(15)	O17–Gd2–O5	97.10(17)
O16–Gd2–O10	139.66(16)	O18–Gd2–O10	75.37(16)
O17–Gd2–O10	76.20(16)	O5– Gd2–O10	125.89(13)
O16–Gd2–O3	79.10(17)	O18–Gd2–O3	82.59(16)

O17–Gd2–O3	125.48(17)	O5–Gd2–O3	122.02(14)
O10–Gd2–O3	103.23(14)	O16–Gd2–O4	78.69(17)
O18–Gd2–O4	113.64(17)	O17–Gd2–O4	77.54(18)
O5–Gd2–O4	159.79(16)	O10–Gd2–O4	72.25(14)
O3–Gd2–O4	52.29(15)	O16–Gd2–O9	130.69(16)
O18–Gd2–O9	74.32(15)	O17–Gd2–O9	70.95(16)
O5–Gd2–O9	74.23(13)	O10–Gd2–O9	52.56(13)
O3–Gd2–O9	149.83(15)	O4–Gd2 –O9	120.88(14)
O16–Gd2–O6	71.97(16)	O18–Gd2–O6	72.26(15)
O17–Gd2–O6	133.82(16)	O5–Gd2–O6	50.91(13)
O10–Gd2–O6	147.59(15)	O3–Gd2–O6	71.15(14)
O4–Gd2–O6	119.95(14)	O9–Gd2–O6	118.07(14)
		8	
O14–Tb1–O13	145.0(2)	O14–Tb1–O8	133.3(2)
O13–Tb1–O8	73.8(2)	O14–Tb1–O15	73.7(2)
O13–Tb1–O15	141.0(2)	O8–Tb1–O15	77.2(2)
O14–Tb1–O2	72.96(19)	O13–Tb1–O2	73.75(18)
O8–Tb1–O2	144.2(2)	O15–Tb1–O2	138.6(2)
O14–Tb1–O3	128.2(2)	O13–Tb1–O3	74.5(2)
O8–Tb1–O3	74.06(19)	O15–Tb1–O3	72.9(2)
O2–Tb1–O3	110.87(18)	O14–Tb1–O4	83.8(2)
O13–Tb1–O4	96.2(2)	O8–Tb1–O4	126.01(19)
O15–Tb1–O4	80.3(2)	O2–Tb1–O4	72.33(17)
O3 –Tb1– O4	52.47(17)	O14–Tb1–O1	74.79(19)
O13–Tb1–O1	76.71(19)	O8–Tb1–O1	104.89(18)
O15–Tb1–O1	136.7(2)	O2–Tb1–O1	52.72(15)
O3–Tb1–O1	150.2(2)	O4–Tb1–O1	124.59(17)
O14–Tb1–O7	85.71(18)	O13–Tb1–O7	104.4(2)
O8–Tb1–O7	52.19(19)	O15–Tb1–O7	76.6(2)
O2–Tb1–O7	124.10(17)	O3–Tb1–O7	122.54(18)
O4–Tb1–O7	156.5(2)	O1–Tb1–O7	72.14(17)
O17–Tb2–O18	70.49(19)	O17–Tb2–O16	143.80(18)
O18–Tb2–O16	143.79(19)	O17–Tb2–O11	81.05(18)
O18–Tb2–O11	97.10(19)	O16 –Tb2–O11	82.51(18)
O17–Tb2–O5	139.47(18)	O18–Tb2–O5	76.18(19)
O16–Tb2–O5	75.18(18)	O11–Tb2–O5	126.16(16)
O17–Tb2–O10	78.46(19)	O18–Tb2–O10	77.2(2)
O16–Tb2–O10	113.9(2)	O11–Tb2–O10	159.47(19)
O5–Tb2–O10	72.13(16)	O17–Tb2–O9	78.97(19)
O18–Tb2–O9	125.47(19)	O16–Tb2–O9	82.73(18)
O11–Tb2–O9	121.76(17)	O5–Tb2–O9	103.35(18)
O10–Tb2–O9	52.71(18)	O17–Tb2–O6	130.47(18)
O18–Tb2–O6	71.02(18)	O16–Tb2–O6	74.17(17)
O11–Tb2–O6	74.05(16)	O5–Tb2–O6	53.00(15)

O10–Tb2–O6	121.06(16)	O9–Tb2–O6	150.23(17)
O17–Tb2–O12	71.92(18)	O18–Tb2–O12	133.89(19)
O16–Tb2–O12	72.63(18)	O11–Tb2–O12	51.15(16)
O5–Tb2–O12	147.74(18)	O10–Tb2–O12	119.80(17)
O9–Tb2–O12	70.65(17)	O6–Tb2–O12	118.13(16)

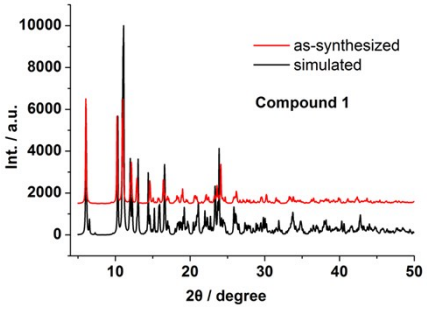

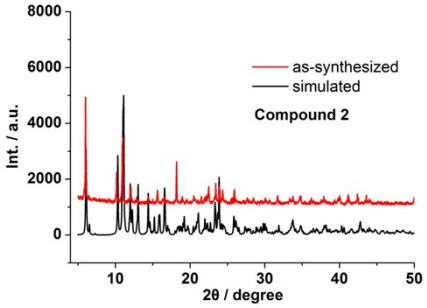

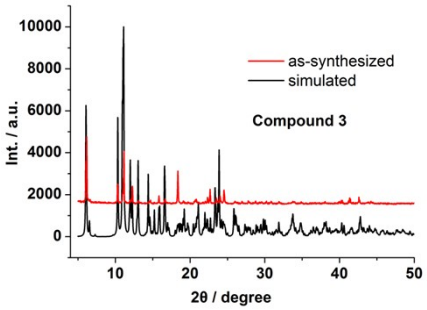

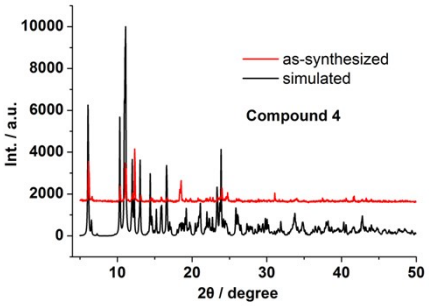
as-synthesized
simulated
Compound 4
Int. / a.u.
2θ / degree

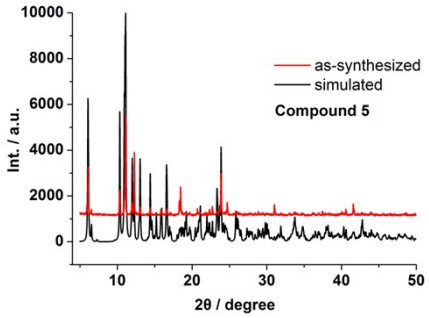
as-synthesized
simulated
Compound 5
Int. / a.u.
2θ / degree

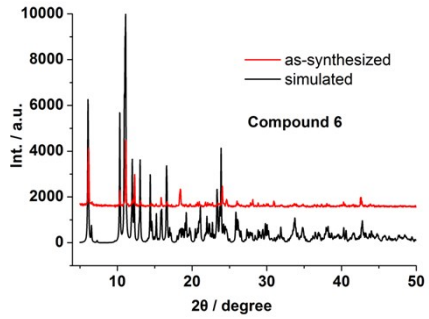
as-synthesized
simulated
Compound 6
Int. / a.u.
2θ / degree

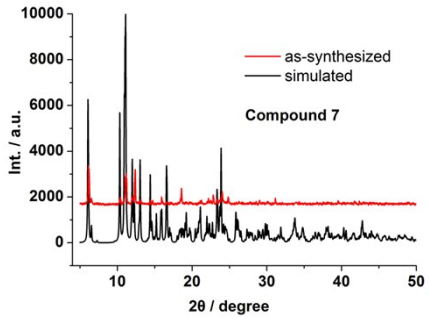
as-synthesized
simulated
Compound 7
Int. / a.u.
2θ / degree

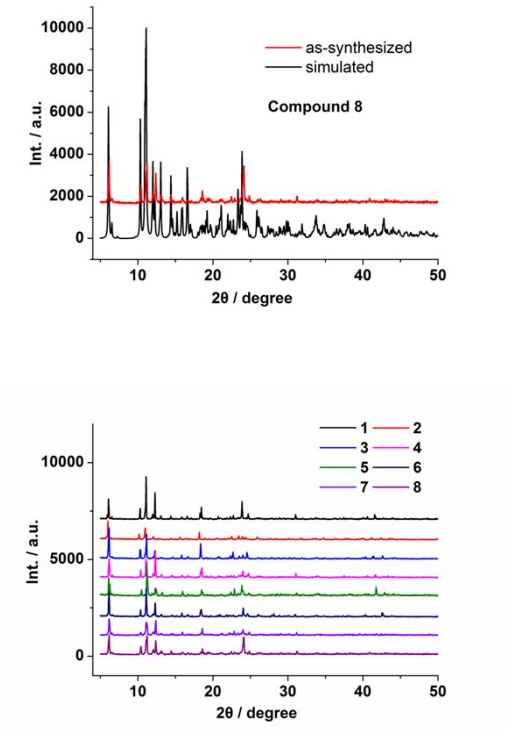

Fig. S4 PXRD patterns of simulated from the X–ray single–crystal structures and as–synthesized samples of **1**–**8** and PXRD patterns of **1–8**.

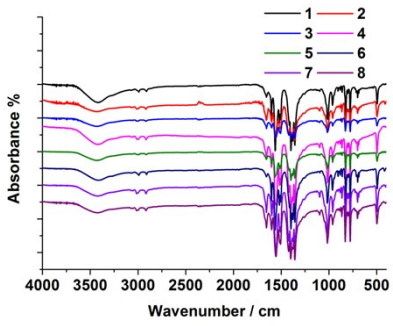

Fig. S5 The IR spectra of **1–8** recorded from a KBr pellet.

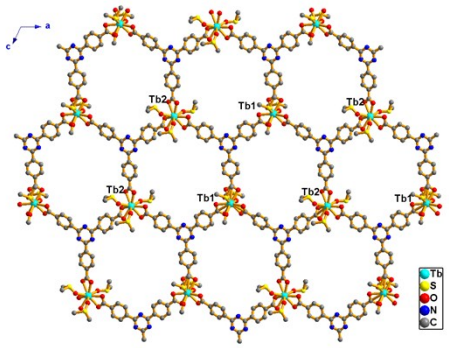

Fig. S6 View of the monolayer in the *ac* plane of **8**.

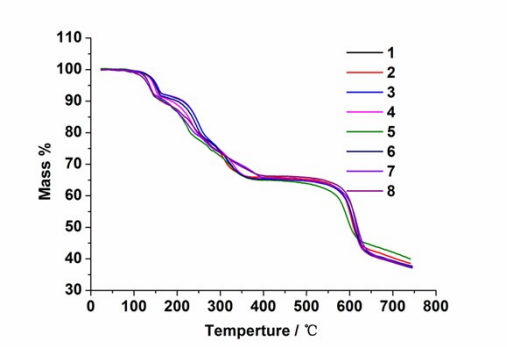

Fig. S7 The TG curves of **1–8**.

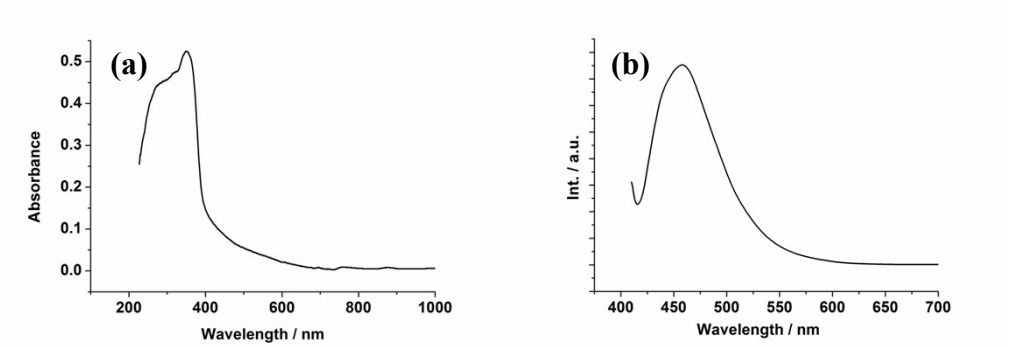

Fig. S8 (a) UV–vis absorption and (b) emission spectra of H_3TATB in solid state at room temperature.

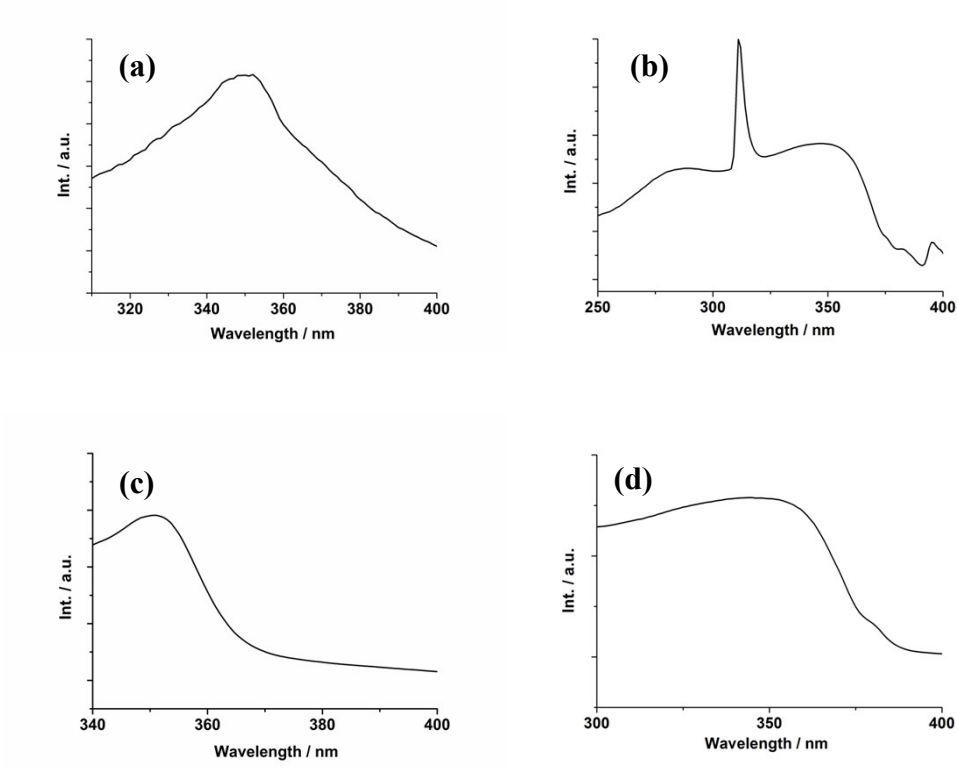

Fig. S9 The excitation spectra of **1** (a), **5** (b), **7** (c) and **8** (d) in solid state at room temperature, monitored at 466 nm, 619 nm, 466 nm and 546 nm, respectively.

Similarly as that of **1**, compound **7** also showes blue luminescence (Fig. 7b and S10(a), ESI†) with the broadband emission centered at 466 nm excited at 350 nm (the excitation spectra is given in Fig. S9(c), ESI†). It may be attributed to the fact that the lowest excited state of Gd^{3+} $^6P_{7/2}$ is too high to accept energy from the ligand, thus its characteristic 4f–4f transition is not visible. Such a broadband emission is also assigned to the intraligand $\pi \leftarrow \pi^*$ transition of $TATB^{3-}$.

The luminescence of compound **2** can be described as a light blue emission (Fig. 7b). It shows two broad emission bands centered at 468 and 490 nm excited at 350 nm (Fig. S10(b), ESI†). The Ce^{3+} ion is the only trivalent lanthanide ion, exhibiting reduction of the energy of 5d states by splitting of the crystal and ligand fields that enables 4f→5d excitation within the UV region close to the visible and 5d→4f emission in the visible region of the spectrum.[1]

As shown in Fig. S10(d), ESI,† compound **4** exhibits orange red light upon excitation at 350 nm (Fig. 7b). The visible emission spectrum consists of three emission bands at 565 nm, 603 nm and 647 nm, attributed to $^4G_{5/2}\rightarrow{}^6H_{5/2}$, $^4G_{5/2}\rightarrow{}^6H_{7/2}$ and $^4G_{5/2}\rightarrow{}^6H_{9/2}$ transitions, respectively. The strongest transition in the visible region is the $^4G_{5/2}\rightarrow{}^6H_{7/2}$ transition. The transition located at 565 nm, $^4G_{5/2}\rightarrow{}^6H_{5/2}$, has a predominant magnetic dipole character.[2] Upon excitation with UV light, we also have observed characteristic emission in the NIR region from the Sm^{3+} ions in compound **4** (Fig. S10(e), ESI†), which is a rarely described phenomenon. All the NIR emission bands come from the $^4G_{5/2}$ excited state, among which the strongest band at 940 nm is assigned to $^4G_{5/2}\rightarrow{}^6F_{5/2}$ transition. Two discernible peaks at 1122 and 1190 nm are suspected to be due to the Stark splitting of $^6F_{9/2}$.[3]

Upon excitation at 350 nm, the NIR emission spectrum of compound **3** can be obtained (Fig. S10(c), ESI†). It is based on a broad emission signal from 800 to 1500 nm with an emission maximum at 1016 nm, and the three bands located at 881nm, 1016nm and 1480 nm are attributed to the transitions from the excited state ($^1D_2$) to the $^3F_2$, $^3F_4$ and $^1G_4$ levels of Pr^{3+} ion, respectively.[4]

The emission spectrum of compound **6** clearly shows three NIR emission bands around 870−913 nm, 1056 and 1331 nm upon excitation at 350 nm (Fig. S10(f), ESI†), corresponding to $^4F_{3/2}\rightarrow{}^4I_{9/2}$, $^4F_{3/2}\rightarrow{}^4I_{11/2}$ and $^4F_{3/2}\rightarrow{}^4I_{13/2}$ transitions, respectively, which belongs to the characteristic emission of Nd^{3+} ions. The $^4F_{3/2}\rightarrow{}^4I_{9/2}$ emission presents splitting, which is mainly attributed to "crystal–field effects" of Nd^{3+} ion in a *C*1 symmetry.[5] Among the three emission bands, the intensity of 1056 nm emission band is the strongest, and for a long time this center has been found to have potential application in laser systems. The 1331 nm band offers the good opportunity to develop new materials (containing Nd^{3+} ion) suitable for the optical amplification operating at 1.3 μm, one of the telecommunication windows.[6]

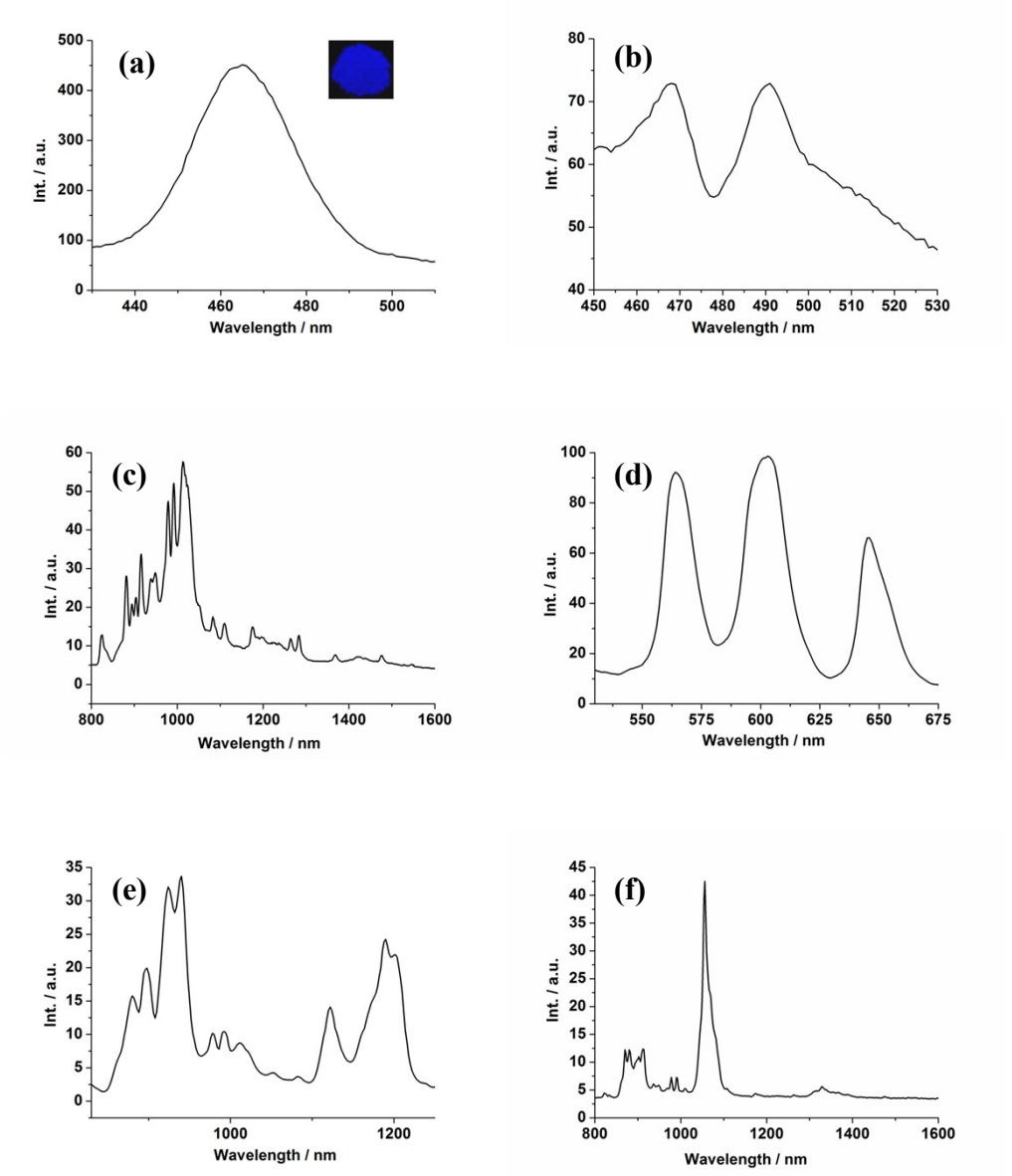

Fig. S10 Emission spectra of **7** (a), **2** (b) and **4** (d); NIR emission spectra of **3** (c), **4** (e) and **6** (f).

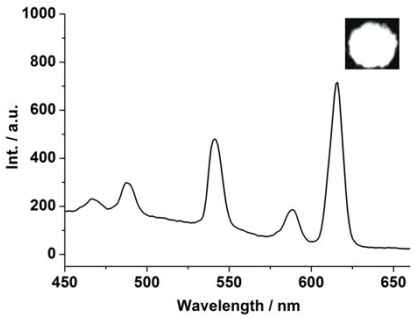

(a)

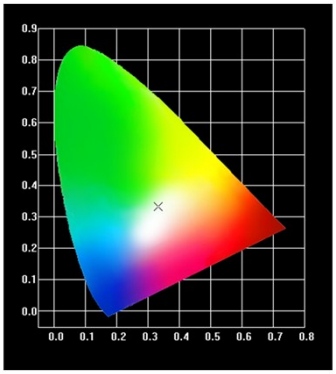

(b)

Fig. S11 (a) Emission spectra and (b) CIE chromaticity diagram for **$Eu_{0.24}Tb_{0.03}La_{0.73}$–TATB** excited at 350 nm.

Table S6 The corresponding CIE coordinates of the $Eu_xTb_yLa_{1-x-y}$–TATB excited at 350nm

	CIE chromaticity coordinates
$Eu_{0.25}Tb_{0.045}La_{0.705}$–TATB	(0.3431, 0.3840)
$Eu_{0.245}Tb_{0.04}La_{0.715}$–TATB	(0.3320, 0.3711)
$Eu_{0.255}Tb_{0.035}La_{0.71}$–TATB	(0.3502, 0.3700)
$Eu_{0.24}Tb_{0.03}La_{0.73}$–TATB	**(0.3323, 0.3349)**
$Eu_{0.235}Tb_{0.02}La_{0.745}$–TATB	(0.2980, 0.3391)

References

1. G. Blasse and B. C. Grabmaier, *Luminescent Materials*, SpringerVerlag, Berlin, Germany, 1994.
2. H. N. Li, H. Y. Li, L. K. Li, L. Xu, K. Hou and S. Q. Zang, *Cryst. Growth Des.*, 2015, **15**, 4331.
3. (a) S. Su, W. Chen, C. Qin, S. Song, Z. Guo, G. Li, X. Song, M. Zhu, S. Wang, Z. Hao and H. Zhang, *Cryst. Growth Des*., 2012, **12**, 1808; (b) K. E. Knope, D. T. de Lill, C. E. Rowland, P. M. Cantos and C. L. Cahill, *Inorg. Chem.*, 2012, **51**,

201.

4. (a) T. J. Foley, B. S. Harrison and A. S. Knefely, *Inorg. Chem.*, 2003, **42**, 5023; (b) L. N. Sun, Y. N. Qiu, T. Liu, J. Feng, W. Deng and L.Y. Shi, *Luminescence*, 2015, **30**, 1071.
5. S. Chen, R. Q. Fan, C. F. Sun, P. Wang, Y. L. Yang, Q. Su and Y. Mu, *Cryst. Growth Des*., 2012, **12**, 1337.
6. L. N. Sun, W. Mai and S. Dang, *J. Mater. Chem.*, 2012, **22**, 5121.